Combustion Theory and Modelling, 2021
https://doi.org/10.1080/13647830.2021.1939166

Effect of Taylor dispersion on the thermo-diffusive instabilities of flames in a Hele–Shaw burner

Joel Daou*

Department of Mathematics, University of Manchester, Manchester, UK

(*Received 18 November 2020; accepted 22 May 2021*)

We investigate the effect of Taylor dispersion on the thermo-diffusive instabilities of premixed flames. This is a physically interesting and analytically tractable problem within a relatively unexplored class of problems pertaining to the interaction between Taylor dispersion (or flow-enhanced diffusion) and Turing-like instabilities in reaction–diffusion systems. The analysis is carried out in the Hele–Shaw burner configuration and adopts a constant density and negligible heat-loss assumptions. These simplifying assumptions allow to isolate the effect of Taylor dispersion on flame stability (by switching off the Darrieus–Landau instability and experimentally challenging extinction phenomena) while keeping the problem analytically tractable. Starting from a 3D formulation, depth-averaged equations are first obtained leading to a 2D model which accounts for enhanced diffusion in the flow direction and shows that diffusion is effectively anisotropic. A linear stability analysis of the travelling wave solutions of the 2D problem leads to a simple dispersion relation which generalises a classical one obtained by Sivashinsky to incorporate the effect of the flow Peclet number coupled to that of the mixture's Lewis number. Based on the new dispersion relation, stability-bifurcation diagrams are drawn in terms of the Peclet and Lewis numbers and their physical implications are discussed. In particular, the study clearly demonstrates the ability of Taylor dispersion to significantly affect the flame thermo-diffusive instabilities, whether these are of the cellular or oscillatory types, with the effect on the latter being more pronounced. It is found that Taylor dispersion typically promotes the cellular instability and hampers the oscillatory instability. This is the first stability analysis accounting for Taylor dispersion in the context of combustion and has thus a fundamental value, both in combustion and in other reaction–diffusion areas, independent of the fact that the phenomena predicted may well be difficult to reproduce experimentally.

Keywords: Taylor dispersion; flame instabilities; Hele–Shaw burner; travelling-waves in reaction–diffusion systems; turing instability

1. Introduction

Taylor dispersion is a well-investigated topic which was initiated by Taylor's seminal paper [1] in which a formula describing the dispersion of a solute in a Poiseuille flow was derived and was later generalised by Aris [2] to parallel flows in tubes with arbitrary cross sections. Taylor-Aris formula is derived under the assumption that the characteristic diffusion transverse time is small compared with the advective time. The derivation shows that the cross-sectionally averaged concentration of the solute obeys a one-dimensional equation with an effective diffusion coefficient D_{eff} which is larger than the diffusion coefficient D

*Email: joel.daou@manchester.ac.uk

This article was originally published with errors, which have now been corrected in the online version. Please see Correction (http://dx.doi.org/10.1080/13647830.2021.1949924)

such that

$$\frac{D_{\text{eff}}}{D} = 1 + \gamma \text{Pe}_D^2 \tag{1}$$

where Pe_D is a Peclet number based on D and γ a numerical coefficient determined by the velocity profile. If u_m is the maximum of the velocity profile, then $\gamma = 1/192$ for a Poiseuille flow in a circular pipe with radius a and Peclet number $\text{Pe}_D = au_m/D$, while $\gamma = 8/945$ for a 2D Poiseuille flow in a channel with half-width h and $\text{Pe}_D = hu_m/D$. Applications of Taylor dispersion are ubiquitous in areas involving transport phenomena and this is reflected by the abundance of related publications in the literature; see the book by Brenner and Edwards [3] for a comprehensive review.

Despite its widespread study, Taylor dispersion has surprisingly not received any dedicated investigation in combustion except in our recent papers [4,5] addressing premixed flames, and even more recently in a paper by Liñán *et al.* [6] addressing diffusion flames. The effect of variable density has been incorporated in the analysis in [4,5], while the effect of preferential diffusion associated with non-unity Lewis numbers has been incorporated in [5,6]. In particular, the analyses revealed that the essential flame characteristics (such as the propagation speed of the premixed flame, and the temperature, location and burning rate of the diffusion flame) are significantly affected by preferential-diffusion effects characterised by an effective Lewis number Le_{eff} which depends on the flow Peclet number. For example, for a premixed flame propagating against a 2D Poiseuille flow, it is found that

$$\frac{\text{Le}_{\text{eff}}}{\text{Le}} = \frac{1 + \gamma(1-\alpha)^2\text{Pe}^2}{1 + \gamma(1-\alpha)^2\text{Pe}^2\text{Le}^2}, \tag{2}$$

where $\text{Le} = D_T/D_F$ is the Lewis number, $\text{Pe} = hu_m/D_T$ the Peclet number, and α the gas expansion parameter defined in terms of the unburnt gas and burnt gas densities ρ_u and ρ_b by $\alpha = 1 - \rho_b/\rho_u$; here and elsewhere D_T and D_F refer to the thermal diffusivity and the fuel diffusion coefficient in a fuel lean mixture, respectively. Formula (2), which can be inferred from (1) in the constant density case $\alpha = 0$, is derived in [5] in the distinguished limit $\epsilon \to 0$ with $\text{Pe} = O(1)$, where $\epsilon \equiv h/\delta_L$ is the channel width h measured with the laminar flame thickness δ_L.

As noted in [5], these flow dependent preferential effects are expected to be an important factor when addressing flame stability. To our knowledge, however, the coupling between flame stability and Taylor dispersion is as yet a totally unexplored topic. The initiation of the exploration of this scientifically rich topic is the main object of the present paper. Our investigation will focus on premixed flames, and more specifically on their thermo-diffusive instabilities which are controlled by preferential diffusion effects [7–9]. The analysis is conveniently conducted in the framework of a Hele–Shaw burner configuration which is amenable to theoretical as well as experimental investigations on flame instabilities as done in [10,11]. For illustration and future reference, a sketch of the experimental setup of [10] is shown in Figure 1 whose captions include a brief description of the operation of the experiment. In actuality, the investigation of flame instabilities is complex even in the rather academic Hele–Shaw configuration, due to the fact that these are wide-ranging and that they typically interact with each other. Such instabilities may include the thermo-diffusive, the Darrieus–Landau, the Rayleigh–Taylor and the Saffman–Taylor instabilities [11–13].

For a thorough overview of the vast topic of flame instabilities, the reader is referred to dedicated reviews, e.g. [14–16]. These highlight in particular two major intrinsic flame

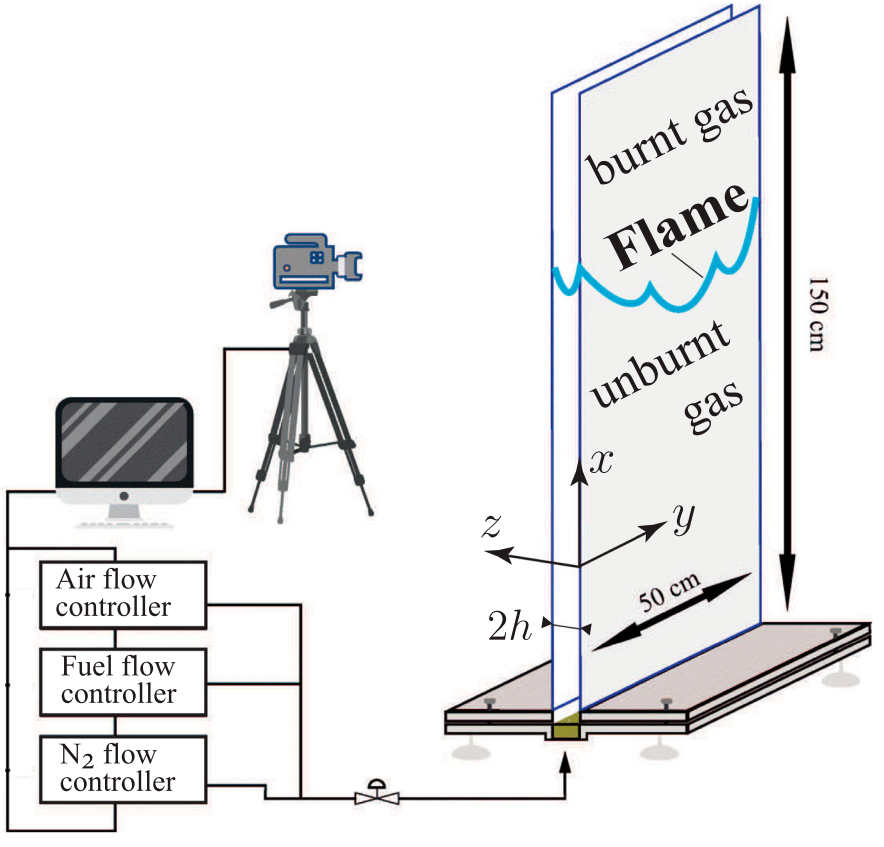

Figure 1. Sketch of Hele–Shaw burner (IRPHE, University of Aix-Marseille) adapted from [10] showing a flame propagating downwards. As described in [10], the burner's operation is briefly as follows. By opening the inlet valve at the bottom, a reactive mixture flows upwards to fill the cell and is ignited at the top of the burner where a flame parallel to the horizontal y-direction is formed and remains anchored thanks to a flow velocity exceeding on average the laminar flame speed S_L. Closing the valve, the flow is stopped and the downwards flame propagation is recorded.

instabilities in premixed combustion. The first, known as the Darrieus–Landau or hydrodynamic instability, is the instability of an interface propagating towards a less dense medium [17]. The second instability, known as the thermo-diffusive instability [7], occurs in fuel-lean mixtures where the thermal diffusivity D_T and the fuel diffusion coefficient D_F are such that their ratio, the Lewis number $\mathrm{Le} = D_T/D_F$, is sufficiently away from unity. In fact, two types of thermo-diffusive instability are distinguished, depending on whether Le is sufficiently larger than unity (where the instability is oscillatory, and occurs through a Hopf-bifurcation) or Le is sufficiently smaller than unity (where the instability is cellular, and occurs through a stationary bifurcation). These two types are collectively referred to herein as thermo-diffusive instabilities, using the plural. The thermo-diffusive instabilities may be identified as Turing-like instabilities [14] since they require, as in the case of Turing instability in a reaction–diffusion system [18], two diffusive processes to have differing diffusion coefficients. Now, since non-unit values of the Lewis number are at the root of the thermo-diffusive instabilities and since Taylor dispersion introduces an effective Lewis

number $\mathrm{Le}_{\mathrm{eff}}$ which is significantly modified by the flow as seen[1] from (2), we expect that Taylor dispersion has significant influence, worth exploring, on the thermo-diffusive instabilities. This is a highly original investigation that is best initiated by addressing the stability of a planar flame adopting the constant density approximation ($\alpha = 0$), which switches off the hydrodynamic instability, and assuming further that all heat-losses are negligible, although these are difficult to ignore experimentally. These simplifying assumptions will allow us to isolate the effect of Taylor dispersion on flame stability while making the problem analytically tractable. The initially unperturbed flame will be taken to be transverse to the flow direction, say parallel to the y-axis in Figure 1 and propagating downwards against an upward flow. Parenthetically, we note that in the experiment of [10] represented in Figure 1, the effect of the flow (or forced convection) has not been addressed. Despite the simplifying assumptions adopted, the problem has still a crucial complication: Taylor dispersion, which leads to enhanced diffusion and to formula (2) for $\mathrm{Le}_{\mathrm{eff}}$, is applicable in the longitudinal direction (x-direction in Figure 1); in the transverse (y-)direction diffusion is unaffected by the flow. Therefore, the stability problem in the x-y plane (obtained by z-averaging the governing equations), is one involving *anisotropic diffusion*. Accordingly, the classical approach of tackling the problem, using familiar jump conditions applicable at inner reaction layers needs significant revision. This revision and related aspects are addressed in this work. The main task is therefore to revisit the premixed flame thermo-diffusive instabilities accounting for the consequences of Taylor dispersion and the corresponding anisotropic diffusion. This task will be carried out analytically, with the principal outcome being the derivation of a dispersion relation describing the linear stability of the planar flame whose implications will be explored.

The presentation is structured as follows. The problem formulation is given in Section 2. Starting from the 3D governing equations for flame propagation between two parallel plates against a Poiseuille flow, a 2D model is derived upon depth-averaging and using perturbation methods. The 2D model incorporates Taylor dispersion in the flow direction and the resulting anisotropic diffusion. The derivation of this model is explained in the text and is supported by Appendix 1 which is included in order to make the paper reasonably self-contained. Section 3 is dedicated to the linear stability analysis of 1D travelling wave solutions of the 2D model, representing specifically planar flames perpendicular to the flow direction. This section contains novel theoretical material, such as the derivation of non-standard jump conditions accounting for non-isotropic diffusion applicable at thin reaction zones, which is supported by a dedicated appendix, Appendix 2. The linear stability analysis culminates in the derivation of a dispersion relation whose implications are examined in Section 4. The paper closes with concluding remarks given in Section 5.

2. Formulation

2.1. *Governing equations and Taylor dispersion*

We consider a flame propagating in a channel of width $2h$ against a Poiseuille flow of amplitude $\hat{A}$ as represented in Figure 2. In a Cartesian frame of reference $(\hat{x}, \hat{y}, \hat{z})$ attached to the walls, the governing equations are

$$\frac{\partial T}{\partial \hat{t}} + \hat{A}\left(1 - \frac{\hat{z}^2}{h^2}\right)\frac{\partial T}{\partial \hat{x}} = D_T\left(\frac{\partial^2 T}{\partial \hat{x}^2} + \frac{\partial^2 T}{\partial \hat{y}^2} + \frac{\partial^2 T}{\partial \hat{z}^2}\right) + \frac{q}{c_p} B Y_F\, e^{-E/RT} \tag{3}$$

$$\frac{\partial Y_F}{\partial \hat{t}} + \hat{A}\left(1 - \frac{\hat{z}^2}{h^2}\right)\frac{\partial Y_F}{\partial \hat{x}} = D_F\left(\frac{\partial^2 Y_F}{\partial \hat{x}^2} + \frac{\partial^2 Y_F}{\partial \hat{y}^2} + \frac{\partial^2 Y_F}{\partial \hat{z}^2}\right) - B Y_F\, e^{-E/RT} \tag{4}$$

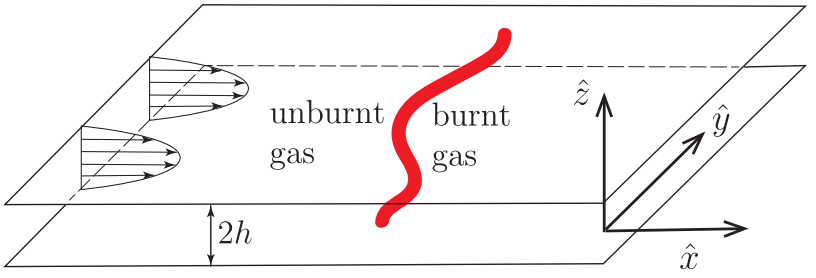

Figure 2. Flame propagation against a parallel flow in Hele–Shaw channel with width $2h$.

and are subject to the boundary conditions

$$\frac{\partial T}{\partial \hat{z}} = \frac{\partial Y_F}{\partial \hat{z}} = 0 \quad \text{at } \hat{z} = \pm h \tag{5}$$

$$T = T_u, \quad Y_F = Y_{Fu} \text{ as } \hat{x} \to -\infty \tag{6}$$

$$T = T_{ad}, \quad Y_F = 0 \text{ as } \hat{x} \to +\infty \tag{7}$$

Here, the flame is modelled by a single chemical reaction whose rate $\hat{\omega}$ follows an Arrhenius law with pre-exponential factor B and activation energy E such that

$$\text{Fuel} \Rightarrow \text{Product} + q, \quad \frac{\hat{\omega}}{\hat{\rho}} = BY_F \exp\left(-\frac{E}{RT}\right)$$

where $\hat{\rho}$ is the density (assumed constant), q the heat release per unit mass of the fuel (assumed to be deficient), R the universal gas constant, Y_F the fuel mass fraction and T the temperature. We denote by $T_{ad} \equiv T_u + qY_{Fu}/c_p$ the adiabatic flame temperature (c_p being the mixture's heat capacity, assumed constant) and use the subscript u (throughout) to indicate values in the unburnt mixture (as $\hat{x} \to -\infty$). For simplicity, the channel is assumed to be of infinite extent in the $\hat{y}$-direction, and we shall simply require that T and Y_F are bounded as $\hat{y} \to \pm\infty$. The walls are assumed rigid and adiabatic and volumetric heat-losses are neglected.

Now, the 3D problem (3)–(7) can be reduced in first approximation to a 2D problem for $\overline{T}$ and $\overline{Y}_F$, where the bar indicates quantities depth-averaged across the channel width $2h$ such that

$$\overline{T} = \overline{T}(\hat{x}, \hat{y}, \hat{t}) = \frac{1}{2h}\int_{-h}^{h} T \, \mathrm{d}\hat{z}$$

This reduction, as explained in Section 2.2 and in Appendix 1, can be obtained using an asymptotic approach similar to that of Daou *et al.* [5] and leads to the governing equations

$$\frac{\partial \bar{T}}{\partial \hat{t}} + \frac{2\hat{A}}{3}\frac{\partial \bar{T}}{\partial \hat{x}} = D_T(1 + \gamma \mathrm{Pe}^2)\frac{\partial^2 \bar{T}}{\partial \hat{x}^2} + D_T\frac{\partial^2 \bar{T}}{\partial \hat{y}^2} + \frac{q}{c_p}B\bar{Y}_F\, e^{-E/R\bar{T}} \tag{8}$$

$$\frac{\partial \bar{Y}_F}{\partial \hat{t}} + \frac{2\hat{A}}{3}\frac{\partial \bar{Y}_F}{\partial \hat{x}} = D_F(1 + \gamma \mathrm{Pe}^2\mathrm{Le}^2)\frac{\partial^2 \bar{Y}_F}{\partial \hat{x}^2} + D_F\frac{\partial^2 \bar{Y}_F}{\partial \hat{y}^2} - B\bar{Y}_F\, e^{-E/R\bar{T}} \tag{9}$$

subject to the boundary conditions

$$\bar{T} = T_u, \quad \bar{Y}_F = Y_{Fu} \text{ as } \hat{x} \to -\infty \tag{10}$$

$$\bar{T} = T_{ad}, \quad \bar{Y}_F = 0 \text{ as } \hat{x} \to +\infty \tag{11}$$

Note that in the 2D problem the Poiseuille flow $\hat{u} \equiv \hat{A}(1 - \hat{z}^2/h^2)$ is replaced by its average value $\bar{\hat{u}} = 2\hat{A}/3$, and the diffusion coefficients D_T and D_F are replaced in the longitudinal direction $\hat{x}$ by effective enhanced values in agreement with Taylor–Aris dispersion formula (1).

It is important to emphasise that the enhancement of diffusion is in the longitudinal $\hat{x}$-direction only, and not in the $\hat{y}$-direction. The problem thus appears as one involving *anisotropic diffusion*.

Our aim is to investigate analytically the stability of the planar flame solutions (independent of $\hat{y}$) of the depth-averaged problem (8)–(11) to small perturbations. That is, we need to revisit the thermo-diffusive instabilities of flames accounting for the consequences of Taylor dispersion and the corresponding anisotropic diffusion.

2.2. *Non-dimensionalisation and the depth-averaged problem*

We begin by non-dimensionalising Equations (3)–(7) by choosing S_L as unit speed, $\delta_L/\hat{A}$ as unit time, h as unit length in the $\hat{z}$-direction, and δ_L as unit length in the $\hat{x}$ and $\hat{y}$ directions. Here,

$$S_L = \sqrt{\frac{2}{\beta^2}\mathrm{Le} D_T Be^{-\frac{E}{RT_{ad}}}} \quad \text{and} \quad \delta_L = \frac{D_T}{S_L} \tag{12}$$

are the laminar flame speed and the planar flame thickness. Thus, in terms of

$$x = \frac{\hat{x}}{\delta_L}, \quad y = \frac{\hat{y}}{\delta_L}, \quad z = \frac{\hat{z}}{h}, \quad t = \frac{\hat{t}}{\delta_L/\hat{A}}, \quad y_F = \frac{Y_F}{Y_{Fu}}, \quad \theta = \frac{T - T_u}{T_{ad} - T_u} \tag{13}$$

the non-dimensional governing equations are

$$\epsilon \mathrm{Pe}\left\{\frac{\partial \theta}{\partial t} + u\frac{\partial \theta}{\partial x}\right\} = \epsilon^2\left\{\frac{\partial^2 \theta}{\partial x^2} + \frac{\partial^2 \theta}{\partial y^2}\right\} + \frac{\partial^2 \theta}{\partial z^2} + \epsilon^2 \omega \tag{14}$$

$$\epsilon \mathrm{Pe}\left\{\frac{\partial y_F}{\partial t} + u\frac{\partial y_F}{\partial x}\right\} = \frac{\epsilon^2}{\mathrm{Le}}\left\{\frac{\partial^2 y_F}{\partial x^2} + \frac{\partial^2 y_F}{\partial y^2}\right\} + \frac{1}{\mathrm{Le}}\frac{\partial^2 y_F}{\partial z^2} - \epsilon^2 \omega \tag{15}$$

and are subject to the boundary conditions

$$\frac{\partial \theta}{\partial z} = \frac{\partial y_F}{\partial z} = 0 \quad \text{at } z = \pm 1 \tag{16}$$

$$\theta = 0, \quad y_F = 1 \text{ as } x \to -\infty \tag{17}$$

$$\theta = 1, \quad y_F = 0 \text{ as } x \to +\infty \tag{18}$$

Here $u \equiv 1 - z^2$ is the scaled Poiseuille flow and ω is the non-dimensional reaction rate given by

$$\omega = \frac{\beta^2}{2\mathrm{Le}} y_F \exp\left(\frac{\beta\,(\theta - 1)}{1 + \alpha_h\,(\theta - 1)}\right) \tag{19}$$

where $\beta \equiv E(T_{ad} - T_u)/RT_{ad}^2$ is the Zeldovich number and $\alpha_h \equiv (T_{ad} - T_u)/T_{ad}$ a heat release coefficient. Furthermore, the non-dimensional parameters appearing in the equations are defined by

$$\epsilon = \frac{h}{\delta_L}, \quad \mathrm{Pe} = \frac{h\hat{A}}{D_T} = \epsilon A, \quad \mathrm{Le} = \frac{D_T}{D_F}$$

and represent, respectively, the (non-dimensional) flow scale, the Peclet number, and the Lewis number.

Now, following the methodology of [5], we integrate Equations (14)–(15) with respect to z across the channel width ($z : -1 \to 1$). Thus, as detailed in Appendix 1, we obtain to leading-order in an asymptotic expansion where $\epsilon \to 0$ and $\mathrm{Pe} = O(1)$, the two-dimensional equations

$$\epsilon \mathrm{Pe}\left\{\frac{\partial \bar{\theta}}{\partial t} + \bar{u}\frac{\partial \bar{\theta}}{\partial x}\right\} = \epsilon^2(1 + \gamma \mathrm{Pe}^2)\frac{\partial^2 \bar{\theta}}{\partial x^2} + \epsilon^2 \frac{\partial^2 \bar{\theta}}{\partial y^2} + \epsilon^2 \omega(\bar{\theta}, \bar{y}_F) \tag{20}$$

$$\epsilon \mathrm{Pe}\left\{\frac{\partial \bar{y}_F}{\partial t} + \bar{u}\frac{\partial \bar{y}_F}{\partial x}\right\} = \frac{\epsilon^2}{\mathrm{Le}}(1 + \gamma \mathrm{Pe}^2 \mathrm{Le}^2)\frac{\partial^2 \bar{y}_F}{\partial x^2} + \frac{\epsilon^2}{\mathrm{Le}}\frac{\partial^2 \bar{y}_F}{\partial y^2} - \epsilon^2 \omega(\bar{\theta}, \bar{y}_F) \tag{21}$$

Here, $\bar{u} = \frac{2}{3}$ and $\omega(\overline{\theta}, \overline{y}_F)$ is given by the rhs of (19) with θ and y_F replaced by $\overline{\theta}$ and $\overline{y}_F$ where the notation

$$\overline{\phi} \equiv \frac{1}{2}\int_{-1}^{1} \phi \, \mathrm{d}z \quad \text{and} \quad \phi' \equiv \phi - \overline{\phi}$$

is used to characterise the depth-average of any quantity ϕ and its fluctuation.

Equations (20)–(21) are supplemented by the boundary conditions

$$\bar{\theta} = 0, \quad \bar{y}_F = 1 \text{ as } x \to -\infty \tag{22}$$

$$\bar{\theta} = 1, \quad \bar{y}_F = 0 \text{ as } x \to +\infty \tag{23}$$

which follow from (16)–(18); as $y \to \pm\infty$ we shall simply require that $\overline{\theta}$ and $\overline{y}_F$ are bounded to complete the mathematical formulation.

2.3. *The planar flame solution in the presence of Taylor-dispersion*

The problem (20)–(23) admits one-dimensional travelling wave solutions of the form $\overline{\theta} = \overline{\theta}(\xi)$ and $\overline{y}_F = \overline{y}_F(\xi)$ where $\xi = x + Ut$ whose stability is the main focus of the investigation. These y-independent traveling waves describe planar flames travelling in the negative x-direction with speed U, with $U > 0$ indicating propagation to the left with respect to the walls. The unknown parameter U and the corresponding solutions are determined from the one-dimensional eigen-boundary value problem

$$U_T \frac{\mathrm{d}\overline{\theta}}{\mathrm{d}\xi} = \left(1 + \gamma \mathrm{Pe}^2\right)\frac{\mathrm{d}^2\overline{\theta}}{\mathrm{d}\xi^2} + \omega(\overline{\theta}, \overline{y}_F) \tag{24a}$$

$$U_T \frac{\mathrm{d}\overline{y}_F}{\mathrm{d}\xi} = \frac{1 + \gamma \mathrm{Pe}^2 \mathrm{Le}^2}{\mathrm{Le}}\frac{\mathrm{d}^2\overline{y}_F}{\mathrm{d}\xi^2} - \omega(\overline{\theta}, \overline{y}_F) \tag{24b}$$

$$\overline{\theta} = 0, \quad \overline{y}_F = 1 \text{ as } \xi \to -\infty \tag{24c}$$

$$\overline{\theta} = 1, \quad \overline{y}_F = 0 \text{ as } \xi \to +\infty \tag{24d}$$

in which

$$U_T \equiv \frac{\mathrm{Pe}}{\epsilon}\,(U+\bar{u}) \quad \left(\text{with} \quad \bar{u}=\frac{2}{3}\right)$$

appears as an eigenvalue describing the propagation speed with respect to the unburnt gas. As done in [5], the solution is given in the limit $\beta \to \infty$ by

$$\overline{\theta} = \begin{cases} \exp \dfrac{U_T \xi}{1+\gamma \mathrm{Pe}^2} \\ 1 \end{cases} \quad , \quad \overline{y}_F = \begin{cases} 1-\exp \dfrac{\mathrm{Le}\, U_T \xi}{1+\gamma \mathrm{Pe}^2 \mathrm{Le}^2} & \text{for } \xi < 0 \\ 0 & \text{for } \xi > 0 \end{cases} \tag{25}$$

with

$$U_T = \frac{1+\gamma \mathrm{Pe}^2}{\left(1+\gamma \mathrm{Pe}^2 \mathrm{Le}^2\right)^{1/2}} \tag{26}$$

3. Linear stability analysis

3.1. *Governing equations and NEF reformulation*

The stability of the planar solution (25) will now be addressed by using the two-dimensional time-dependent equations

$$\frac{\partial \overline{\theta}}{\partial \tau} + U_T \frac{\partial \overline{\theta}}{\partial \xi} = \left(1+\gamma \mathrm{Pe}^2\right) \frac{\partial^2 \overline{\theta}}{\partial \xi^2} + \frac{\partial^2 \overline{\theta}}{\partial y^2} + \omega(\overline{\theta}, \overline{y}_F) \tag{27}$$

$$\frac{\partial \overline{y}_F}{\partial \tau} + U_T \frac{\partial \overline{y}_F}{\partial \xi} = \left(1+\gamma \mathrm{Pe}^2 \mathrm{Le}^2\right) \mathrm{Le}^{-1} \frac{\partial^2 \overline{y}_F}{\partial \xi^2} + \mathrm{Le}^{-1} \frac{\partial^2 \overline{y}_F}{\partial y^2} - \omega(\overline{\theta}, \overline{y}_F) \tag{28}$$

which are obtained by applying the change of variables $\xi = x + Ut$, $y = y$ and $\tau = \epsilon t/\mathrm{Pe}$ to Equations (20)–(21). The equations are to be solved together with the boundary conditions (24c)–(24d) and the requirement of boundedness of $\overline{\theta}$ and $\overline{y}_F$ as $y \to \pm\infty$.

The stability analysis is most consistently carried out in the limit $\beta \to \infty$ using the so-called near-equidiffusional flame (NEF) approximation [19, p. 33]. The approximation is based on the assumption that the Lewis number deviates little from unity such that $\mathrm{Le} \sim 1 + l/\beta$ with l being an $O(1)$ quantity referred to as the reduced Lewis number. In the NEF approximation, we may introduce the expansions

$$\bar{\theta} \sim \theta^0 + \frac{\theta^1}{\beta}, \quad \bar{y}_F \sim y_F^0 + \frac{y_F^1}{\beta} \tag{29}$$

and reformulate the problem in terms of the leading order temperature θ^0 and the quantity $h \equiv \theta^1 + y_F^1$. The reformulated problem consists in solving the equations

$$\theta_\tau^0 + U_T \theta_\xi^0 = \left(1+\gamma \mathrm{Pe}^2\right) \theta_{\xi\xi}^0 + \theta_{yy}^0 \tag{30}$$

$$h_\tau + U_T h_\xi = \left(1+\gamma \mathrm{Pe}^2\right) h_{\xi\xi} + h_{yy} + l\left[\left(1-\gamma \mathrm{Pe}^2\right) \theta_{\xi\xi}^0 + \theta_{yy}^0\right] \tag{31}$$

which are applicable outside an infinitely thin reaction sheet, given by $\xi = f(y,\tau)$ say, subject to the boundary conditions

$$\theta^0 = 0, \quad h = 0 \text{ as } \xi \to -\infty \tag{32}$$

$$\theta^0 = 1, \quad h = 0 \text{ as } \xi \to +\infty \tag{33}$$

and the jump conditions

$$[\![\theta^0]\!] = 0, \quad [\![h]\!] = 0 \tag{34}$$

$$[\![h_\xi]\!] + \frac{1 + f_y^2 - \gamma \mathrm{Pe}^2}{1 + f_y^2 + \gamma \mathrm{Pe}^2}\, l\, [\![\theta_\xi^0]\!] = 0 \tag{35}$$

$$\sqrt{1 + f_y^2 + \gamma \mathrm{Pe}^2}\; [\![\theta_\xi^0]\!] = -\exp\left(\frac{h}{2}\right) \tag{36}$$

applicable at $\xi = f(y,\tau)$. Here $[\![\,\phi\,]\!] = \phi(\xi = f^+) - \phi(\xi = f^-)$ denotes a jump in the value of a quantity ϕ across the sheet. The derivation of jumps conditions (34)–(36) is provided in Appendix 2 along with a justification of the NEF formulation of this subsection. We note that these jump conditions, accounting for anisotropic diffusion, are novel and that their use is not limited to the stability analysis under consideration. Their derivation follows however a methodology commonly used in premixed (see, e.g. [19, p. 39], [20, p. 527] and [21]) and partially-premixed [22,23] combustion, which is based on an inner analysis using a stretched variable such as $\bar{\zeta} = \beta(\xi - f(y,\tau))$ used in Appendix 2; the jump conditions result then from the matching conditions between the inner and outer profiles. We note that conditions (34)–(36) reduce to the well known jump conditions of premixed flames [20, p. 527] when $\gamma \mathrm{Pe}^2 = 0$, that is when Taylor dispersion is absent.

We are now in a position to investigate the stability of the planar flame solution (denoted by a tilde), which is governed by Equations (30)–(36) with $\partial/\partial\tau = 0$ and $\partial/\partial y = 0$. The solution is given by

$$\tilde{f} = 0,\ \tilde{\theta} = \begin{cases} \exp \dfrac{\xi}{\left(1 + \gamma \mathrm{Pe}^2\right)^{1/2}} \\ 1 \end{cases},$$

$$\tilde{h} = \begin{cases} \dfrac{-1 + \gamma \mathrm{Pe}^2}{\left(1 + \gamma \mathrm{Pe}^2\right)^{3/2}} l\xi \exp \dfrac{\xi}{\left(1 + \gamma \mathrm{Pe}^2\right)^{1/2}} & \text{for } \xi < 0 \\ 0 & \text{for } \xi > 0 \end{cases} \tag{37}$$

and

$$U_T = \sqrt{1 + \gamma \mathrm{Pe}^2}$$

and these expressions can also be obtained from (25) and (26) in the limit $\beta \to \infty$ using the fact that $\mathrm{Le} \sim 1 + l/\beta$ and $h \sim \beta(\overline{\theta} + \overline{y}_F - 1)$.

A normal-mode stability analysis can now be applied to the basic solution (37) by considering perturbations of the form

$$[f, \theta^0, h] = [0, \tilde{\theta}(\xi), \tilde{h}(\xi)] + \delta\, e^{s\tau + iky}[1, \hat{\theta}(\xi), \hat{h}(\xi)] \tag{38}$$

where δ is a small number representing the amplitude of the perturbation, and k and s are a real and a complex numbers representing its wavelength and its growth rate, respectively. The main aim is to derive a dispersion relation expressing the dependence of s on k and the parameters l and $\gamma \mathrm{Pe}^2$ of the problem, i.e. a relationship of the form

$$F(s, k; l, \gamma \mathrm{Pe}^2) = 0 \tag{39}$$

Instability will correspond of course to situations for which $Re(s) > 0$ occurs.

3.2. *Derivation of the dispersion relation*

This section is dedicated to the derivation of the explicit form of the dispersion relation (39). The methodology used is similar to that used in the literature, e.g. [9], [19, p. 50], [20, p. 532] and [21].

When perturbed solutions of the form (38) are substituted into Equations (30)–(36), an eigen-boundary value problem for the functions $\hat{\theta}(\xi)$ and $\hat{h}(\xi)$ is obtained. Namely, with primes denoting differentiation with respect to ξ, we have

$$(1+\gamma \mathrm{Pe}^2)\hat{\theta}'' - U_T\hat{\theta}' - (s+k^2)\hat{\theta} = 0 \tag{40}$$

$$(1+\gamma \mathrm{Pe}^2)\hat{h}'' - U_T\hat{h}' - (s+k^2)\hat{h} = -l\left\{\left(1-\gamma \mathrm{Pe}^2\right)\hat{\theta}'' - k^2\hat{\theta}\right\} \tag{41}$$

for $\xi \neq 0$, subject to the boundary conditions

$$\hat{\theta} = 0, \quad \hat{h} = 0 \text{ as } \xi \to \pm\infty \tag{42}$$

and the jump conditions

$$\left[\!\left[\hat{\theta}\right]\!\right] = \frac{1}{\sqrt{1+\gamma \mathrm{Pe}^2}}, \quad \left[\!\left[\hat{h}\right]\!\right] = -\frac{l\left(1-\gamma \mathrm{Pe}^2\right)}{\left(1+\gamma \mathrm{Pe}^2\right)^{\frac{3}{2}}} \tag{43}$$

$$\left[\!\left[\hat{h}'\right]\!\right] + \frac{1-\gamma \mathrm{Pe}^2}{1+\gamma \mathrm{Pe}^2}\, l \left[\!\left[\hat{\theta}'\right]\!\right] = -\frac{\left(1-\gamma \mathrm{Pe}^2\right) l}{\left(1+\gamma \mathrm{Pe}^2\right)^2} \tag{44}$$

$$\left[\!\left[\hat{\theta}'\right]\!\right] = \frac{1}{1+\gamma \mathrm{Pe}^2} - \frac{\hat{h}(0^+)}{2\left(1+\gamma \mathrm{Pe}^2\right)^{\frac{1}{2}}} \tag{45}$$

at $\xi = 0$. It is to be noted that the jump conditions at the reaction sheet $\xi = f(y,\tau)$ have been transferred to $\xi = 0$, using Taylor expansions for small values of δ, since $f = O(\delta)$ according to (38). The solution of the linear second-order differential Equations (40)–(41) subject to all conditions except (44) is found to be

$$\hat{\theta} = \begin{cases} -\dfrac{\exp\left(r^+\xi\right)}{\left(1+\gamma \mathrm{Pe}^2\right)^{\frac{1}{2}}} \\ 0 \end{cases},$$

$$\hat{h} = \begin{cases} \left[\dfrac{1-\Gamma}{\left(1+\gamma \mathrm{Pe}^2\right)^{\frac{1}{2}}} + \dfrac{l\left(1-\gamma \mathrm{Pe}^2\right)}{\left(1+\gamma \mathrm{Pe}^2\right)^{\frac{3}{2}}} + l\,\chi\,\xi\right] \exp\left(r^+\xi\right) & \text{for } \xi < 0 \\ \dfrac{1-\Gamma}{\left(1+\gamma \mathrm{Pe}^2\right)^{\frac{1}{2}}} \exp\left(r^-\xi\right) & \text{for } \xi > 0 \end{cases}$$

where

$$\Gamma = \sqrt{1+4(s+k^2)}, \quad r^{\pm} = \frac{1\pm\Gamma}{2\sqrt{1+\gamma \mathrm{Pe}^2}} \quad \text{and}$$

$$\chi = \frac{(\Gamma+1+2s)\left(1-\gamma \mathrm{Pe}^2\right) - 4\gamma \mathrm{Pe}^2 k^2}{2\Gamma\left(1+\gamma \mathrm{Pe}^2\right)^2}$$

In deriving the solution above, unstable modes characterised by $\mathrm{Re}(s) \geq 0$ are assumed; this assumption implies that $\mathrm{Re}(\Gamma) \geq 1$, and hence $\mathrm{Re}(r^+) \geq 0$, and $\mathrm{Re}(r^- \leq 0)$.[2] Use of these expressions in the jump condition (44) leads, after simple manipulations, to the dispersion relation

$$2\Gamma^2(\Gamma - 1) + \frac{l}{1 + \gamma \mathrm{Pe}^2}\left[(\Gamma - 1 - 2s)(1 - \gamma \mathrm{Pe}^2) + 4\gamma \mathrm{Pe}^2 k^2\right] = 0 \tag{46}$$

We note that this equation reduces to the dispersion relation derived by Sivashinsky [9] when $\gamma \mathrm{Pe}^2 = 0$, as it should.

4. Implications of the findings

The main outcome of this study is the derivation of the dispersion relation (46), which encapsulates all the information characterising the linear stability of the flame to arbitrary small perturbations. As usual, the perturbations are taken as linear combination of normal modes, with each mode being here proportional to an amplitude depending on ξ multiplied by $\exp(s\tau + iky)$ where k is the mode's wave number and s its growth rate. In this relation, the notation $\Gamma = \sqrt{1 + 4s + 4k^2}$ is used and two parameters are involved, namely the reduced Lewis number $l = \beta(\mathrm{Le} - 1)$ and the combination $\gamma \mathrm{Pe}^2$ characterising the parallel flow.

We note that the dispersion relation incorporates the effect of Taylor dispersion and the resulting anisotropy of diffusion. For illustration, a sample of the results implied by the dispersion relation is shown in Figure 3 for selected values of the parameter $\gamma \mathrm{Pe}^2$, where the stability regions are identified in the l-k plane along with the bifurcation curves separating them from the instability regions. For a selected value of $\gamma \mathrm{Pe}^2$, a given point (l, k) is in a stability region (shaded) if $Re(s) < 0$ for all corresponding roots $s = s(k; l, \gamma \mathrm{Pe}^2)$ of the dispersion relation. By sweeping the l-k plane systematically, the complex roots $s = s(k; l, \gamma \mathrm{Pe}^2)$ are determined numerically using Maple. The instability regions are unshaded and correspond to the condition $Re(s) > 0$ being satisfied by at least one root s. The bifurcation curves correspond to either $s = 0$ (stationary bifurcation) or $Re(s) = 0$ with $Im(s) \neq 0$ (Hopf bifurcation). Equation (46) implies that the stationary bifurcation curve has the explicit expression

$$l = \frac{\left(-2 - 8k^2\right)\left(\sqrt{1 + 4k^2} - 1\right)\left(1 + \gamma \mathrm{Pe}^2\right)}{\sqrt{1 + 4k^2} - 1 + \gamma \mathrm{Pe}^2\left(1 + 4k^2 - \sqrt{1 + 4k^2}\right)} \tag{47}$$

When $\gamma \mathrm{Pe}^2 = 0$, we recover the classical results (see, e.g. [9] and [20, p. 535]) with a stationary bifurcation curve obtained for sufficiently negative values of l and a Hopf bifurcation curve for sufficiently large positive values; this is illustrated in the top left subfigure of Figure 3. The stationary bifurcation curve, given in this case by $l = -2 - 8k^2$, determines the onset of the so-called flame cellular instability which occurs a l is decreased below a critical value $l_c = -2$. The Hopf bifurcation curve determines the onset of the so-called flame oscillatory instability which occurs when l is increased beyond a critical value $l_h = \frac{32}{3}$. In the domain $l_c < l < l_h$, the flame is thermo-diffusively stable.

As $\gamma \mathrm{Pe}^2$ is increased the Hopf bifurcation curve is displaced to the right and disappears when $\gamma \mathrm{Pe}^2 > 1$. This is more clearly seen in Figure 4 where the Hopf bifurcation curve is

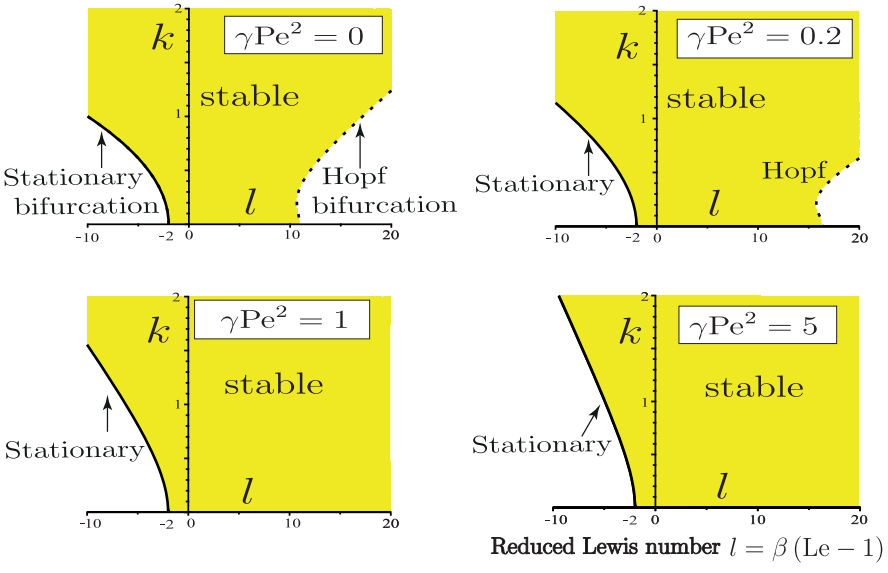

Figure 3. Stability regions and bifurcation curves in the l–k plane for selected values of the parameter $\gamma \mathrm{Pe}^2$; l is the reduced Lewis number and k is the perturbation wave number.

plotted in the l-k plane for selected values of the parameter $\gamma \mathrm{Pe}^2$. Thus a sufficiently strong flow impedes the flame oscillatory instability. Also, the size of the stability region in the left half-plane (delimited from the left by the stationary bifurcation curve) is reduced by an increase in $\gamma \mathrm{Pe}^2$ which indicates that the flow typically promotes the cellular instability. Note however that the stationary bifurcation curves all originate from the point $(l, k) = (-2, 0)$, which indicates that the onset of the cellular instability as l is decreased still corresponds to $l_c = -2$, irrespective of the valued of $\gamma \mathrm{Pe}^2$. This conclusion is true provided the domain size L_y in the y-direction is infinite, as assumed here, so as to permit the mode $k = 0$ corresponding to an infinite wavelength perturbation. In actual domains with finite size L_y, the onset of instability will correspond to values of l_c less than -2 which are increasing functions of $\gamma \mathrm{Pe}^2$; that is, it is easier to trigger the thermo-diffusive instability when Taylor dispersion is accounted for. This follows from the fact that the stationary bifurcation curve given by (47) moves upwards in the (l, k)-plane as $\gamma \mathrm{Pe}^2$ is increased as seen in Figure 3, although it always originates from the point $(l, k) = (-2, 0)$.

Another way of consolidating the conclusions of the last two paragraphs is to determine the stability regions and bifurcation curves in the l-$\gamma \mathrm{Pe}^2$ plane or equivalently the Le-$\gamma \mathrm{Pe}^2$ plane. This is done in Figure 5 where the stability domain appears shaded and the bifurcation curves, represented by solid lines, are clearly labelled. These correspond to a domain infinitely large in the y-direction, $L_y = \infty$, as assumed in this study. Note parenthetically however that one may infer from the dispersion relation how the bifurcation curves delimiting the stability region are changed when L_y is finite and suitable lateral boundary conditions assumed (say at $y = \pm L_y/2$). For example, continuing to neglect heat-losses and assuming Neumann (or zero-flux) lateral boundary conditions at $y = \pm L_y/2$ implies that k must take discrete values which are multiples of $k_{min} = \pi/L_y$. The bifurcation curves can then be recomputed using the dispersion relation and k_{min}. For illustration, the recomputed curves are plotted in Figure 4 for the case $L_y = 5$ as a dotted line for the

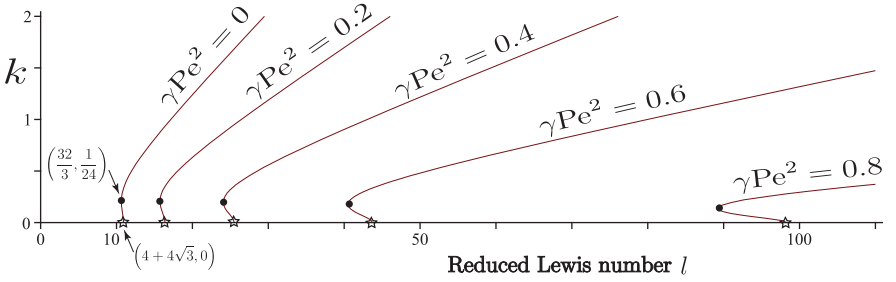

Figure 4. Hopf bifurcation curves in the l–k plane for selected values of the parameter γPe^2; l is the reduced Lewis number and k is the perturbation wave number. The full circles determine the critical conditions for the onset of the oscillatory instability which are also reported in Figure 5. The stars indicate the intersection of the bifurcation curves with the $k = 0$ axis and characterise the onset of instability of a planar flame to planar perturbations; these have the analytical expression $l = (4 + 4\sqrt{3})(1 + \gamma Pe^2)/(1 - \gamma Pe^2)$.

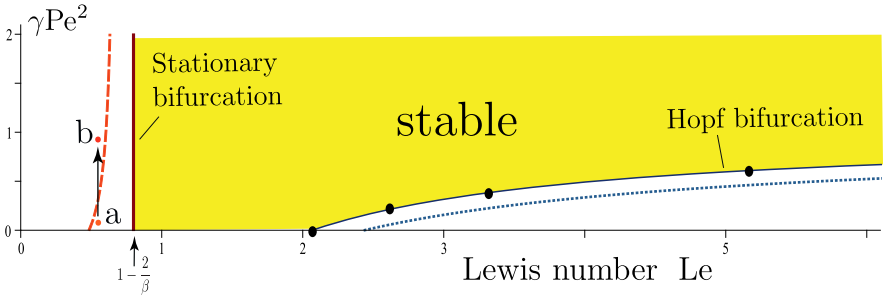

Figure 5. Stability regions and bifurcation curves in the Le-γPe^2 plane; $Le = 1 + l/\beta$ with $\beta = 10$ being adopted here. The full circles on the Hopf bifurcation curve determine the critical conditions for the onset of the oscillatory instability which are also reported in Figure 4. The stationary bifurcation curve reduces to the vertical line $Le = 1 - 2/\beta$ or $l = -2$. The stable domain is shaded. Parenthetically, to illustrate the effect of a bounded domain in the y-direction, the bifurcations curves are also plotted for the case $L_y = 5$ for which the minimum permitted value of k is $k_{min} = \pi/5$. In this case, the Hopf bifurcation and stationary bifurcation curves are represented by the dotted and dashed curves, respectively. Also in this case, a stable configuration (corresponding, e.g. to point a) may become unstable (point b) by an increase in γPe^2 (Taylor dispersion) as represented by the vertical arrow.

Hopf bifurcation and a dashed line for the stationary bifurcation. It is interesting to note that in this case situations occur for which the effect of the flow (or Taylor-dispersion) is destabilising, in the sense that an increase in the value of γPe^2 can lead from a stable configuration (corresponding, e.g. to point a in the figure) to an unstable configuration (point b).

As a last comment regarding the effect of Taylor dispersion on the stability of the flame, we note that the dispersion relation (46) has always a real root $s(k)$ such that $s(0) = 0$ (which is a consequence of the translational invariance of the problem in the longitudinal ξ direction) and the Taylor expansion of $s(k)$ for small values of k^2 is given by

$$s = -\left(1 + \frac{l}{2}\right)k^2 - \frac{l^2\left(6 - l + (6 + l)\gamma Pe^2\right)}{8 + 8\gamma Pe^2}k^4 + O(k^6)$$

It is this root which is at the origin of the cellular instability whose onset is seen to correspond to $l = l_c = -2$ irrespective of the value of the flow parameter $\gamma \mathrm{Pe}^2$. In the weakly unstable regime near the onset of instability, $l \lessapprox l_c$, the expansion above can be written as

$$s = -\left(1 + \frac{l}{2}\right) k^2 - \frac{4 + 2\gamma \mathrm{Pe}^2}{1 + \gamma \mathrm{Pe}^2} k^4 + \ldots$$

and implies the following linear evolution equation for the flame front $f(y, \tau) \propto e^{s\tau + iky}$:

$$f_\tau = \left(1 + \frac{l}{2}\right) f_{yy} - \frac{4 + 2\gamma \mathrm{Pe}^2}{1 + \gamma \mathrm{Pe}^2} f_{yyyy}$$

This equation reduces, as it should, to the linear Kuramoto–Sivashinsky equation when $\gamma \mathrm{Pe}^2 = 0$. The coefficient of the fourth derivative f_{yyyy} being negative, the last term is stabilising as in Sivashinsky's original equation [9]. Note however that this term is most stabilising when the flow is absent as its coefficient is most negative, equal to -4, when $\gamma \mathrm{Pe}^2 = 0$ and increases monotonically to -2 as $\gamma \mathrm{Pe}^2$ increases towards infinity. For weakly unstable flames, $l \lessapprox -2$, the unstable modes are those with wavenumbers k such that

$$0 < k^2 < -\frac{1 + \gamma \mathrm{Pe}^2}{8 + 4\gamma \mathrm{Pe}^2} (l + 2)$$

and the most amplified mode is characterised by a wavenumber k_0 and a growth rate s_0 given by

$$k_0^2 = -\frac{1 + \gamma \mathrm{Pe}^2}{16 + 8\gamma \mathrm{Pe}^2} (l + 2), \quad s_0 = \frac{1 + \gamma \mathrm{Pe}^2}{64 + 32\gamma \mathrm{Pe}^2} (l + 2)^2$$

Thus an increase in $\gamma \mathrm{Pe}^2$ widens the range of unstable wavenumbers and increases the maximum growth rate and has therefore a destabilising effect.

5. Conclusion

To conclude, we note that our analysis demonstrates the ability of Taylor dispersion to significantly affect the flame thermo-diffusive instabilities. This is true whether these are cellular, where Taylor dispersion is found to promote the instability, or oscillatory, where it is found to strongly hamper the instability. The findings are highly original in combustion theory since, to our knowledge, the interaction of Taylor dispersion with flame instabilities do not seem to have been addressed before. For the sake of analytical tractability and in order to isolate the effect of Taylor dispersion, strong assumptions, including the neglect of density variations and heat losses, have been adopted. This has allowed a full analytical treatment culminating in the derivation of a compact dispersion relation which led to transparent conclusions. The study may therefore serve as a new building bloc to incorporate in future investigations addressing flame instabilities in a Hele–Shaw burner under a more general framework which may include, as done in [12,13], the Darrieus–Landau, the Rayleigh–Taylor and the Saffman–Taylor instabilities. In such future investigations, which will build on interesting studies motivated by recent experiments on flame instabilities in Hele–Shaw cells [10,11], our assumptions can be relaxed and the effect of forced convection necessary for Taylor dispersion incorporated.

As a final remark, it is worth pointing out the value of the present study extends well beyond combustion, as it provides an analytical description of the effect Taylor dispersion may have on Turing-like instabilities of propagating fronts in reaction–diffusion systems, such as the 'liquid-flames' in iodate-arsenous acid systems considered by Ronney [24]. More generally, the ability of Taylor dispersion to influence Turing-like instabilities in reaction–diffusion systems seems to be a poorly investigated topic, at least analytically, and deserves in depth exploration in particular in relation to propagating fronts.

Notes

1. Note that formula (2) implies that $\mathrm{Le}_{\mathrm{eff}} \to \mathrm{Le}$ as $\mathrm{Pe} \to 0$ and $\mathrm{Le}_{\mathrm{eff}} \to \mathrm{Le}^{-1}$ as $\mathrm{Pe} \to \infty$
2. Defined as a square root of a complex number, Γ is assumed to lie on the right half-complex plane.

Disclosure statement

No potential conflict of interest was reported by the author(s).

Funding

The author is grateful to the EPSRC for financial support under grant [EP/V004840/1].

References

[1] G.I. Taylor, *Dispersion of soluble matter in solvent flowing slowly through a tube*, Proc. R. Soc. Lond. A. Math. Phys. Sci. 219 (1953), pp. 186–203.
[2] R. Aris, *On the dispersion of a solute in a fluid flowing through a tube*, Proc. R. Soc. Lond. A. Math. Phys. Sci. 235 (1956), pp. 67–77.
[3] H. Brenner and D. Edwards, *Macrotransport processes*, Butterworth-Heinemann, 1993.
[4] P. Pearce and J. Daou, *Taylor dispersion and thermal expansion effects on flame propagation in a narrow channel*, J. Fluid. Mech. 754 (2014), pp. 161.
[5] J. Daou, P. Pearce, and F. Al-Malki, *Taylor dispersion in premixed combustion: Questions from turbulent combustion answered for laminar flames*, Phys. Rev. Fluids 3 (2018), pp. 023201.
[6] A. Liñán, P. Rajamanickam, A.D. Weiss, and A.L. Sánchez, *Taylor-diffusion-controlled combustion in ducts*. Combust. Theory Model. 24 (2020), pp. 1–16.
[7] G. Markstein, *Cell structure of propane flames burning in tubes*, J. Chem. Phys. 17 (1949), pp. 428–429.
[8] G. Sivashinsky, *Diffusional-thermal theory of cellular flames*, Combust. Sci. Technol. 15 (1977), pp. 137–145.
[9] G. Sivashinsky, *Nonlinear analysis of hydrodynamic instability in laminar flames-i. Derivation of basic equations*, AcAau 4 (1977), pp. 1177–1206.
[10] E. Al Sarraf, C. Almarcha, J. Quinard, B. Radisson, and B. Denet, *Quantitative analysis of flame instabilities in a Hele–Shaw burner*, Flow Turbulence Combus. 101 (2018), pp. 851–868.
[11] D. Fernández-Galisteo, V.N. Kurdyumov, and P.D. Ronney, *Analysis of premixed flame propagation between two closely-spaced parallel plates*, Combust. Flame. 190 (2018), pp. 133–145.
[12] G. Joulin and G. Sivashinsky, *Influence of momentum and heat losses on the large-scale stability of quasi-2d premixed flames*, Combust. Sci. Technol. 98 (1994), pp. 11–23.
[13] S. Kang, S.W. Baek, and H. Im, *Effects of heat and momentum losses on the stability of premixed flames in a narrow channel*, Combust. Theory Model. 10 (2006), pp. 659–681.
[14] J. Buckmaster, *The structure and stability of laminar flames*, Annu. Rev. Fluid. Mech. 25 (1993), pp. 21–53.
[15] G.I. Sivashinsky, *Instabilities, pattern formation, and turbulence in flames*, Annu. Rev. Fluid. Mech. 15 (1983), pp. 179–199.

[16] M. Matalon, *Intrinsic flame instabilities in premixed and nonpremixed combustion*, Annu. Rev. Fluid Mech. 39 (2007), pp. 163–191.
[17] L. Landau, *On the theory of slow combustion*, in *Acta Physicochim (USSR)*, 1944, p. 19.
[18] A. Turing, *The chemical basis of morphogenesis*, Phil. Trans. R. Soc. B 237 (1952), pp. 37–47.
[19] J. Buckmaster and G. Ludford, *Lectures on Mathematical Combustion*, Society for Industrial Mathematics, Philadelphia, 1987.
[20] G. Joulin and P. Vidal, *An introduction to the instability of flames, shocks and detonations*, in *Hydrodynamics and Nonlinear Instabilities*, C. Godreche and P. Manneville, eds., Collection Alea-Saclay: Monographs and Texts in Statistical Physics, Cambridge University Press, Cambridge, 1998.
[21] J. Daou, *Premixed flames with a reversible reaction: Propagation and stability*, Combust. Theory Model. 12 (2008), pp. 349–365.
[22] J. Daou, *Asymptotic analysis of flame propagation in weakly-strained mixing layers under a reversible chemical reaction*, Combust. Theory Model. 13 (2009), pp. 189–213.
[23] J. Daou and R. Daou, *Flame balls in mixing layers*, Combust. Flame. 161 (2014), pp. 2015–2024.
[24] P.D. Ronney, *Some open issues in premixed turbulent combustion*, in *Modeling in Combustion Science*, Springer, 1995, pp. 1–22.

Appendices

Appendix 1. Derivation of Taylor dispersion formula

The objective of this appendix is to describe how the 3D problem (3)–(7) can be reduced to the depth-averaged 2D problem (8)–(11) or equivalently to the non-dimensional 2D problem (20)–(23). This demonstrates in particular the enhancement of diffusion in the longitudinal x-direction as predicted by Taylor–Aris dispersion formula (1).

We begin by non-dimensionalising the 3D problem (3)–(7) as done in section 2.2 to obtain (14)–(18) which we rewrite for convenience

$$\epsilon \mathrm{Pe}\left\{\frac{\partial\theta}{\partial t}+u\frac{\partial\theta}{\partial x}\right\}=\epsilon^2\left\{\frac{\partial^2\theta}{\partial x^2}+\frac{\partial^2\theta}{\partial y^2}\right\}+\frac{\partial^2\theta}{\partial z^2}+\epsilon^2\omega \tag{A1}$$

$$\epsilon \mathrm{Pe}\left\{\frac{\partial y_F}{\partial t}+u\frac{\partial y_F}{\partial x}\right\}=\frac{\epsilon^2}{\mathrm{Le}}\left\{\frac{\partial^2 y_F}{\partial x^2}+\frac{\partial^2 y_F}{\partial y^2}\right\}+\frac{1}{\mathrm{Le}}\frac{\partial^2 y_F}{\partial z^2}-\epsilon^2\omega \tag{A2}$$

$$\frac{\partial\theta}{\partial z}=\frac{\partial y_F}{\partial z}=0 \quad \text{at } z=\pm 1 \tag{A3}$$

$$\theta=0, \quad y_F=1 \text{ as } x\to-\infty \tag{A4}$$

$$\theta=1, \quad y_F=0 \text{ as } x\to+\infty \tag{A5}$$

Here $u\equiv 1-z^2$ is the scaled Poiseuille flow and $\omega=\omega(\theta,y_F)$ is a function of two variables representing the nondimensional reaction rate as given by (19). We now introduce for any quantity ϕ its depth-average $\overline{\phi}$ and its fluctuation ϕ' such that

$$\overline{\phi}\equiv\frac{1}{2}\int_{-1}^{1}\phi\,\mathrm{d}z, \quad \phi'\equiv\phi-\overline{\phi} \quad \text{and} \quad \overline{\phi'}=0$$

On integrating (A1) with respect to z and using (A3) we thus obtain

$$\epsilon \mathrm{Pe}\left\{\frac{\partial\bar{\theta}}{\partial t}+\bar{u}\frac{\partial\bar{\theta}}{\partial x}+\overline{u'\frac{\partial\theta'}{\partial x}}\right\}=\epsilon^2\left\{\frac{\partial^2\bar{\theta}}{\partial x^2}+\frac{\partial^2\bar{\theta}}{\partial y^2}\right\}+\epsilon^2\overline{\omega(\theta,y_F)} \tag{A6}$$

where $\overline{u}=\frac{2}{3}$ and $u'=\frac{1}{3}-z^2$. Anticipating that the fluctuations θ' and y_F' are small, of order $\epsilon\mathrm{Pe}$ as we shall confirm below, we may use the Taylor expansion

$$\omega(\theta,y_F)=\omega(\bar{\theta},\bar{y}_F)+\theta'\omega_\theta(\bar{\theta},\bar{y}_F)+y_F'\omega_{y_F}(\bar{\theta},\bar{y}_F)+O(\theta'^2,\theta' y_F',y_F'^2) \tag{A7}$$

to obtain upon depth-averaging

$$\overline{\omega(\theta, y_F)} = \omega(\bar{\theta}, \overline{y_F}) + O(\theta'^2, \theta' y'_F, y'^2_F)$$

Neglecting the quadratic terms in this equation, we can replace $\overline{\omega(\theta, y_F)}$ in (A6) by $\omega(\bar{\theta}, \overline{y_F})$ to obtain

$$\epsilon \mathrm{Pe} \left\{ \frac{\partial \bar{\theta}}{\partial t} + \bar{u} \frac{\partial \bar{\theta}}{\partial x} + \overline{u' \frac{\partial \theta'}{\partial x}} \right\} = \epsilon^2 \left\{ \frac{\partial^2 \bar{\theta}}{\partial x^2} + \frac{\partial^2 \bar{\theta}}{\partial y^2} \right\} + \epsilon^2 \omega(\bar{\theta}, \overline{y_F}) \tag{A8}$$

In order to evaluate the expression $\overline{u' \partial \theta'/\partial x}$ in (A8) in terms of depth-averaged quantities, we need an equation for the fluctuation θ'. This is readily obtained by subtracting (A8) from (A1), and reusing (A7) with the $O(\theta'^2, \theta' y'_F, y'^2_F)$-terms neglected:

$$\epsilon \mathrm{Pe} \left\{ \frac{\partial \theta'}{\partial t} + u' \frac{\partial \bar{\theta}}{\partial x} + u \frac{\partial \theta'}{\partial x} - \overline{u' \frac{\partial \theta'}{\partial x}} \right\} = \frac{\partial^2 \theta'}{\partial z^2} + \epsilon^2 \left\{ \frac{\partial^2 \theta'}{\partial x^2} + \frac{\partial^2 \theta'}{\partial y^2} + \theta' \omega_\theta(\bar{\theta}, \bar{y}_F) + y'_F \omega_{y_F}(\bar{\theta}, \bar{y}_F) \right\}$$

We now consider the double limit $\epsilon \to 0$ with $\epsilon \mathrm{Pe} \to 0$, which is more general than the distinguished limit $\epsilon \to 0$ with $\mathrm{Pe} = O(1)$ used in [5] and mentioned in the text. On the RHS of the equation above only the first term is clearly dominant in the limit $\epsilon \to 0$. On the LHS a single term is dominant in the curly bracket, namely $u' \partial \bar{\theta}/\partial x$, since it is the only term not containing the fluctuation θ' which is assumed small. Hence we have the leading order balance

$$\epsilon \mathrm{Pe}\, u' \frac{\partial \bar{\theta}}{\partial x} = \frac{\partial^2 \theta'}{\partial z^2}$$

This implies that $\theta' = O(\epsilon \mathrm{Pe})$ as anticipated above, and this justifies in particular our neglect of all terms containing θ' on the LHS in the limit $\epsilon \mathrm{Pe} \to 0$. We can now find θ' by integrating the last equation twice w.r.t z, using the boundary conditions $\partial \theta'/\partial z = 0$ at $z = \pm 1$ implied by (A3), the requirement that $\overline{\theta'} = 0$, and the fact that $u' = \frac{1}{3} - z^2$ to obtain

$$\theta' = \epsilon \mathrm{Pe} \frac{\partial \bar{\theta}}{\partial x} \left(\frac{z^2}{6} - \frac{z^4}{12} - \frac{7}{180} \right)$$

From this formula it readily follows that

$$\overline{u' \frac{\partial \theta'}{\partial x}} = -\gamma\, \epsilon \mathrm{Pe} \frac{\partial^2 \bar{\theta}}{\partial x^2} \quad \text{where } \gamma = \frac{8}{945}$$

which allows (A8) to be rewritten as

$$\epsilon \mathrm{Pe} \left\{ \frac{\partial \bar{\theta}}{\partial t} + \bar{u} \frac{\partial \bar{\theta}}{\partial x} \right\} = \epsilon^2 (1 + \gamma \mathrm{Pe}^2) \frac{\partial^2 \bar{\theta}}{\partial x^2} + \epsilon^2 \frac{\partial^2 \bar{\theta}}{\partial y^2} + \epsilon^2 \omega(\bar{\theta}, \bar{y}_F) \tag{A9}$$

Proceeding in the same fashion with the y_F-equation (A3) we obtain similarly

$$\epsilon \mathrm{Pe} \left\{ \frac{\partial \bar{y}_F}{\partial t} + \bar{u} \frac{\partial \bar{y}_F}{\partial x} \right\} = \frac{\epsilon^2}{\mathrm{Le}} (1 + \gamma \mathrm{Pe}^2 \mathrm{Le}^2) \frac{\partial^2 \bar{y}_F}{\partial x^2} + \frac{\epsilon^2}{\mathrm{Le}} \frac{\partial^2 \bar{y}_F}{\partial y^2} - \epsilon^2 \omega(\bar{\theta}, \bar{y}_F) \tag{A10}$$

The boundary conditions for the last two equations follow readily from depth-averaging (A4)–(A5) and are given by

$$\bar{\theta} = 0, \quad \bar{y}_F = 1 \text{ as } x \to -\infty \tag{A11}$$

$$\bar{\theta} = 1, \quad \bar{y}_F = 0 \text{ as } x \to +\infty \tag{A12}$$

We note that Equations (A9)–(A12) are identical to those of the non-dimensional problem (20)–(23). Furthermore, on returning to dimensional variables, it is straightforward to show using (13) that the problem is equivalent to the depth-averaged dimensional problem (8)–(11). This fulfills the objective of this appendix which is precisely to derive the depth-averaged governing equations. In particular, these demonstrate the enhancement of diffusion in the longitudinal x-direction, in agreement with Taylor–Aris dispersion formula (1). Specifically, in the longitudinal direction, the heat and mass diffusion coefficients D_T and D_F, and their ratio defining the Lewis number $\mathrm{Le} = D_T/D_F$, are replaced by effective values (indicated by the subscript eff) given by

$$\frac{D_{T,\mathrm{eff}}}{D_T} = 1 + \gamma \mathrm{Pe}^2, \quad \frac{D_{F,\mathrm{eff}}}{D_F} = 1 + \gamma \mathrm{Pe}^2 \mathrm{Le}^2, \quad \frac{\mathrm{Le}_{\mathrm{eff}}}{\mathrm{Le}} = \frac{1 + \gamma \mathrm{Pe}^2}{1 + \gamma \mathrm{Pe}^2 \mathrm{Le}^2} \tag{A13}$$

Appendix 2. Jump conditions across the reaction sheet

The objective of this appendix is to derive the jumps conditions (34)–(36) and to justify the near-equidiffusional flame (NEF) formulation (30)–(36) of the problem.

We begin by noting that the chemical reaction is confined to a thin region of thickness $O(\beta^{-1})$ which reduces to a surface given by $\xi = f(y,\tau)$ in the limit $\beta \to \infty$. Next we introduce the coordinate $\zeta = \xi - f(y,\tau)$ which is equal to zero at the reaction sheet separating two outer zones known as the preheat zone ($\zeta < 0$) and the burnt gas zone ($\zeta > 0$). Under the change of variables $(\xi, y, \tau) \to (\zeta, y, \tau)$ which implies that

$$\partial_\xi \to \partial_\zeta, \quad \partial_y \to \partial_y - f_y \partial_\zeta, \quad \partial_\tau \to \partial_\tau - f_\tau \partial_\zeta \tag{A14}$$

Equations (27)–(28) become

$$\frac{\partial \overline{\theta}}{\partial \tau} + \left(U_T - f_\tau + f_{yy}\right) \frac{\partial \overline{\theta}}{\partial \zeta} = \left(1 + f_y^2 + \gamma \mathrm{Pe}^2\right) \frac{\partial^2 \overline{\theta}}{\partial \zeta^2} + \frac{\partial^2 \overline{\theta}}{\partial y^2} - 2 f_y \frac{\partial^2 \overline{\theta}}{\partial \zeta \, \partial y} + \omega(\overline{\theta}, \overline{y}_F) \tag{A15}$$

$$\frac{\partial \overline{y}_F}{\partial \tau} + \left(U_T - f_\tau + \frac{f_{yy}}{\mathrm{Le}}\right) \frac{\partial \overline{y}_F}{\partial \zeta} = \frac{1}{\mathrm{Le}} \left\{ \left(1 + f_y^2 + \gamma \mathrm{Pe}^2 \mathrm{Le}^2\right) \frac{\partial^2 \overline{y}_F}{\partial \zeta^2} + \frac{\partial^2 \overline{y}_F}{\partial y^2} - 2 f_y \frac{\partial^2 \overline{y}_F}{\partial \zeta \, \partial y} \right\} - \omega(\overline{\theta}, \overline{y}_F) \tag{A16}$$

These equations are subject to boundary conditions (24c)–(24d) with the limit $\zeta \to \pm\infty$ replacing $\xi \to \pm\infty$. Now, in the NEF approximation where $\mathrm{Le} = 1 + l/\beta$, it is seen by adding (A15) and (A16) so as to eliminate the reaction term and taking into account the boundary conditions that $\overline{\theta} + \overline{y}_F \sim 1$ as $\beta \to \infty$ and that $h = \beta(\overline{\theta} + \overline{y}_F - 1)$ is an order one quantity satisfying

$$\frac{\partial h}{\partial \tau} + \left(U_T - f_\tau + f_{yy}\right) \frac{\partial h}{\partial \zeta} = \left(1 + f_y^2 + \gamma \mathrm{Pe}^2\right) \frac{\partial^2 h}{\partial \zeta^2} + \frac{\partial^2 h}{\partial y^2} - 2 f_y \frac{\partial^2 h}{\partial \zeta \, \partial y} + l \left\{ \left(1 + f_y^2 - \gamma \mathrm{Pe}^2\right) \frac{\partial^2 \overline{\theta}}{\partial \zeta^2} + \frac{\partial^2 \overline{\theta}}{\partial y^2} - 2 f_y \frac{\partial^2 \overline{\theta}}{\partial \zeta \, \partial y} - f_{yy} \frac{\partial \overline{\theta}}{\partial \zeta} \right\} \tag{A17}$$

Note from its derivation that this h-equation, which justifies (31), is valid everywhere in the domain, including the reaction zone, and may be used to replace Equation (A16) for $\overline{y}_F$, since $\overline{y}_F = 1 - \overline{\theta} + h/\beta$. In the outer region outside the reaction zone, the reaction term ω may be neglected to all orders in β^{-1} and the problem is governed by Equations (A15)–(A16), or equivalently (27)–(28), with ω deleted. These chemistry-free equations determine the outer profiles $\overline{\theta}^{\mathrm{outer}}$ and $\overline{y}_F^{\mathrm{outer}}$ described by the outer expansions (29). Alternatively, the outer profiles are determined by (30) (which follows to leading order from (27) with ω set to zero) and the h-equation (31).

The outer profiles, governed by Equations (30)–(31) as we have just explained, are subject to jump conditions (34)–(36) that we now justify. Jump conditions (34) express simply the continuity of the dependent variables across the reaction sheet; this follows in fact from the matching between the inner and outer solutions as we shall demonstrate below. Jump condition (35) can be derived by integration of Equation (A17) across the reaction sheet, namely from $\zeta = 0^-$ to $\zeta = 0^+$, which yields

$$\left(1 + f_y^2 + \gamma \mathrm{Pe}^2\right) \left[\!\left[\frac{\partial h}{\partial \zeta} \right]\!\right]_{\zeta=0^-}^{0^+} + l \left(1 + f_y^2 - \gamma \mathrm{Pe}^2\right) \left[\!\left[\frac{\partial \overline{\theta}}{\partial \zeta} \right]\!\right]_{\zeta=0^-}^{0^+} = 0$$

Note that the right-hand side of the equation above has been set to zero using the continuity of $\bar{\theta}$ and h and hence of their partial derivatives with respect to τ and y across the reaction sheet.

To justify finally jump condition (36), we turn now to the inner solution by introducing an inner variable $\bar{\zeta}$ and inner expansions by

$$\bar{\zeta} = \frac{\zeta}{\beta^{-1}}, \quad \bar{\theta}^{\mathrm{inner}} \sim 1 + \frac{\Theta^1(\bar{\zeta}, y, \tau)}{\beta}, \quad \bar{y}_F^{\mathrm{inner}} \sim \frac{F^1(\bar{\zeta}, y, \tau)}{\beta}$$

The inner problem to leading order is then given by

$$\left(1+f_y^2+\gamma \mathrm{Pe}^2\right)\frac{\partial^2\Theta^1}{\partial\bar{\zeta}^2}+\frac{F^1}{2\mathrm{Le}}\exp\left(\Theta^1\right)=0 \tag{A18}$$

$$\frac{1}{\mathrm{Le}}\left(1+f_y^2+\gamma \mathrm{Pe}^2\mathrm{Le}^2\right)\frac{\partial^2 F^1}{\partial\bar{\zeta}^2}-\frac{F^1}{2\mathrm{Le}}\exp\left(\Theta^1\right)=0 \tag{A19}$$

$$\Theta^1=\theta^1(\zeta=0^+),\quad F^1=0 \text{ as } \bar{\zeta}\to+\infty \tag{A20}$$

$$\Theta^1=\theta^1(\zeta=0^-)+\bar{\zeta}\left.\frac{\partial\theta^0}{\partial\zeta}\right|_{\zeta=0^-},\quad F^1=y_F^1(\zeta=0^-)+\bar{\zeta}\left.\frac{\partial y_F^0}{\partial\zeta}\right|_{\zeta=0^-}\quad\text{as}\quad\bar{\zeta}\to-\infty \tag{A21}$$

We note that conditions (A20) and (A21) follow from the matching requirement

$$\left(\overline{\theta}^{\text{inner}},\overline{y}_F^{\text{inner}}\right)\left(\bar{\zeta}\to\pm\infty\right)=\left(\overline{\theta}^{\text{outer}},\overline{y}_F^{\text{outer}}\right)\left(\zeta\to0^{\pm}\right)$$

In particular, the zeroth-order matching is insured by requiring $\overline{\theta}^{\text{outer}}(0\pm)=1$ and $\overline{y}_F^{\text{outer}}(0\pm)=0$. This implies the continuity of θ^0 across the reaction sheet as expressed in the first equality in (34). Also, the first-order matching is insured by the requirements (A20) and (A21).

The inner problem can now be simplified further, by noting that

$$F^1=\frac{\mathrm{Le}\left(1+f_y^2+\gamma \mathrm{Pe}^2\right)}{\left(1+f_y^2+\gamma \mathrm{Pe}^2\mathrm{Le}^2\right)}\left(\theta^1(\zeta=0^+)-\Theta^1\right)$$

identically; this is seen by adding (A18) to (A19) and using (A20). Equation (A21) then implies that $\theta^1(\zeta=0^+)=\theta^1(\zeta=0^-)$ and $y_F^1(\zeta=0^+)=y_F^1(\zeta=0^-)$ and hence the continuity of h at reaction sheet, that is the second equality in (34).

Eliminating F^1, the inner problem becomes

$$2\left(1+f_y^2+\gamma \mathrm{Pe}^2\mathrm{Le}^2\right)\frac{\partial^2\Theta^1}{\partial\bar{\zeta}^2}+\left(\theta^1|_{\zeta=0^+}-\Theta^1\right)\exp\Theta^1=0 \tag{A22}$$

$$\Theta^1\left(\bar{\zeta}\to-\infty\right)=\theta^1|_{\zeta=0^+}+\bar{\zeta}\left.\frac{\partial\theta^0}{\partial\zeta}\right|_{\zeta=0^-},\quad\Theta^1\left(\bar{\zeta}\to\infty\right)=\theta^1|_{\zeta=0^+} \tag{A23}$$

We now multiply Equation (A22) by $\partial\Theta^1/\partial\bar{\zeta}$ and integrate with respect to $\bar{\zeta}$ from $\bar{\zeta}=-\infty$ to $\bar{\zeta}=+\infty$ to obtain

$$\left(1+f_y^2+\gamma \mathrm{Pe}^2\mathrm{Le}^2\right)\left[\left(\frac{\partial\Theta^1}{\partial\bar{\zeta}}\right)^2\right]_{\bar{\zeta}=-\infty}^{+\infty}+\int_{\Theta^1|_{\bar{\zeta}=-\infty}}^{\Theta^1|_{\bar{\zeta}=+\infty}}\left(\theta^1|_{\zeta=0^+}-\Theta^1\right)\exp\left(\Theta^1\right)\mathrm{d}\Theta^1=0$$

Hence, using (A23), we have

$$\left(1+f_y^2+\gamma \mathrm{Pe}^2\mathrm{Le}^2\right)\left(0-\left.\left(\frac{\partial\theta^0}{\partial\zeta}\right)^2\right|_{\zeta=0^-}\right)+\int_{-\infty}^{\theta^1|_{\zeta=0^+}}\left(\theta^1|_{\zeta=0^+}-\Theta^1\right)\exp\left(\Theta^1\right)\mathrm{d}\Theta^1=0$$

Since the integral in this equation evaluates to $\exp(\theta^1|_{\zeta=0^+})$, we have

$$\left(1+f_y^2+\gamma \mathrm{Pe}^2\mathrm{Le}^2\right)^{\frac{1}{2}}\left.\frac{\partial\theta^0}{\partial\zeta}\right|_{\zeta=0^-}=\exp\left(\frac{\theta^1|_{\zeta=0^+}}{2}\right)$$

Equation (36) follows readily from this equation by noting that the partial derivative with respect to ζ can be replaced by the partial derivative with respect to ξ on account of (A14), that $\zeta=0$ corresponds to $\xi=f$, that Le can be replaced by unity in this leading order formula within the NEF approximation, and that $\theta_\zeta^0|_{\zeta=0^+}=0$ since $\theta^0=1$ identically for $\zeta>0$ or $\xi>f$.